



Abundance, distribution, and feeding ecology of *Pyrosoma atlanticum* in the Northern California Current

Julie B. Schram^{1,*}, Hilarie L. Sorensen¹, Richard D. Brodeur²,
Aaron W. E. Galloway¹, Kelly R. Sutherland¹

¹Oregon Institute of Marine Science, University of Oregon, Charleston, Oregon 97420, USA

²Northwest Fisheries Science Center, National Marine Fisheries Service, National Oceanic and Atmospheric Administration, Newport, Oregon 97366, USA

ABSTRACT: During 2016–2018, unprecedented aggregations of the colonial pelagic tunicate *Pyrosoma atlanticum* were observed in the Northern California Current (NCC). Pyrosomes are common in tropical and sub-tropical ocean waters, but little is known about their abundance, distribution, and trophic ecology in mid-latitude systems. To assess these factors, pyrosomes were collected during cruises in the NCC in May and August 2017. A generalized additive model (GAM) was used to identify relationships between *in situ* environmental variables (temperature, salinity, fluorescence) and distribution and abundance patterns of pyrosomes in May 2017. Fatty acid (FA) profiles were then characterized as diet indicators, and bulk stable isotope analysis of carbon and nitrogen was used to examine spatial variations in potential food sources and trophic level. The GAM identified sea surface temperature and surface salinity as significant variables related to pyrosome densities. The most abundant FA in the pyrosomes was docosahexanoic acid (22:6 ω 3), which serves in pelagic systems as a biomarker for dinoflagellates. Common FA biomarkers for bacteria, carnivory, and dinoflagellates differed by latitude, suggesting that pyrosomes have different diets over a broad latitudinal range. The $\delta^{15}\text{N}$ values of *P. atlanticum* indicate that pyrosomes may be feeding at a relatively low trophic level compared to other zooplankton groups in this region. Offshore pyrosomes had lower $\delta^{13}\text{C}$ values than those collected on the shelf, suggesting incorporation of nearshore carbon in pyrosome tissues. Previously documented rapid reproduction and growth of pyrosomes coupled with efficient feeding behavior for common NCC plankters may support their continued presence in this mid-latitude region.

KEY WORDS: Pyrosoma · Pelagic tunicates · Biomarker · Fatty acids · Stable isotopes · C:N

Resale or republication not permitted without written consent of the publisher

1. INTRODUCTION

The California Current is one example of a variable physical environment that can influence population dynamics along the western coast of the USA, and is one of the major eastern boundary currents that flows equatorward starting from southern British Columbia (around 50° N) to Baja California (30° N). Episodic and seasonal upwelling supports a biologi-

cally productive area and a fisheries hotspot (Checkley & Barth 2009). The Northern California Current (NCC; 42–48° N) is an ideal system to study the relationships between environmental variables and gelatinous zooplankton due to dynamic seasonal upwelling, which is sensitive to regional oceanographic indices and drives biological productivity (Bograd et al. 2009). In the NCC, seasonal and interannual environmental variability (temperature, salinity, dis-

*Corresponding author: jschram@uoregon.edu

solved oxygen [DO], fluorescence) can lead to the development of optimal conditions that support blooms of gelatinous zooplankton including cnidarian jellyfish and pelagic tunicates (Suchman et al. 2012, Miller et al. 2019). Frequent blooms and broader distributions of certain gelatinous zooplankters have been observed in many marine ecosystems, including the NCC (Purcell et al. 2007, Brotz et al. 2012, Zeman et al. 2018), and these blooms can have lasting impacts on ecosystem dynamics and human activities (Purcell et al. 2007, Graham et al. 2014).

Climate regimes in the North Pacific (periods of 1–3 decades) influence pelagic ecosystem dynamics through changes in sea surface temperature (SST), salinity, DO, and currents (Du & Peterson 2018 and citations therein). All of these factors drive the spatial and temporal distribution of species in a given area. In the NCC, major oceanographic phenomena such as the El Niño-Southern Oscillation (ENSO) and Pacific Decadal Oscillation exert strong influence on zooplankton populations (Peterson et al. 2017). There has been a global increase in the frequency and intensity of specific marine heatwave events (Oliver et al. 2018). For example, anomalously warm ocean conditions in the North Pacific, referred to as ‘the Blob’, began in 2013 (Bond et al. 2015, Di Lorenzo & Mantua 2016). The 1–4°C warming of ocean temperatures continued through 2015 followed by a major ENSO event in 2016 (Jacox et al. 2016, Peterson et al. 2017). The effects of these warmer ocean temperatures at the ecosystem scale are not fully understood (Bond et al. 2015), especially as previous reports have documented a link between colder conditions and increased gelatinous zooplankton abundance in some situations (Lynam et al. 2004). However, warming has generally been linked to an increase in frequency of occurrence and abundance of several species of gelatinous zooplankton including pelagic tunicates and cnidarians in the NCC (Brodeur et al. 2017, Peterson et al. 2017, Miller et al. 2019).

Prior to 2014, pyrosomes were not observed in the NCC; however, from 2016–2018, unprecedented aggregations of the colonial pelagic tunicate *Pyrosoma atlanticum* were observed in coastal waters from Oregon to British Columbia (Brodeur et al. 2017, 2019a, Sutherland et al. 2018, Miller et al. 2019). Pyrosomes are common in tropical and sub-tropical ocean waters (Van Soest 1981), but very little is known about their abundance, distribution, and trophic ecology in mid-latitude systems (Sutherland et al. 2018), and what initiated the recent range expansion into the NCC is unclear (Brodeur et al. 2017). Above-

average water temperatures influenced by recent regional environmental conditions from 2013 due to the anomalous warm Blob (Bond et al. 2015), followed by a strong El Niño (Jacox et al. 2016) may have facilitated pyrosome influx and success in the NCC. Rapid reproduction and growth have previously been documented in pyrosomes, and this capability, coupled with their efficient feeding behavior, may support their continued presence in this area (Sutherland et al. 2018, Miller et al. 2019).

Pyrosomes (Greek for ‘fire bodies’) are holoplanktonic grazers comprised of zooids encased in a gelatinous tunic made primarily of cellulose (Godeaux 1998). Pyrosome colony size ranges from <1 cm to several meters in length, and the number of zooids can reach 20 000 per colony in ~1 m long colonies (Décima et al. 2019). Zooids have a branchial basket lined with cilia, and the beating of these cilia pulls water in through the oral siphon and out through the atrial siphon. Water flow drives both feeding and locomotion, and a mucous mesh lining the branchial basket efficiently captures planktonic microorganisms (Alldredge & Madin 1982, Godeaux 1998).

The few studies that have examined pyrosome diet have indicated that pyrosomes feed primarily on phytoplankton, including diatoms, dinoflagellates, prymnesiophytes, and coccolithophores (Culkin & Morris 1970, Drits et al. 1992, Perissinotto et al. 2007). Pyrosomes have high clearance rates of up to 35 l colony⁻¹ h⁻¹ (Drits et al. 1992, Perissinotto et al. 2007), which enables them to potentially impact food web interactions by outcompeting other planktonic grazers (Drits et al. 1992). When pyrosomes form dense aggregations, they are capable of reducing phytoplankton standing stock by >50% in surface waters (Drits et al. 1992). Beyond the few previously published diet studies based on identification of gut contents, little is known about the trophic ecology of pyrosomes. Pyrosomes are difficult to keep alive in the laboratory for feeding experiments and, due to the small size and rapid digestion of their phytoplankton prey, visual gut content analysis using microscopy techniques is challenging.

Trophic biomarkers including fatty acids (FAs) are often used to study food web dynamics of marine organisms to identify feeding habits and trophic position (Dalsgaard et al. 2003, Pitt et al. 2008). Many primary producers have distinct FA markers or multivariate FA ‘signatures’ and therefore can characterize the diet and identify trophic connections of organisms (Perissinotto et al. 2007, Pitt et al. 2008, Kelly & Scheibling 2012, Tilves et al. 2018). Proportions of FAs and ratios between certain FAs can also help

determine dominance of certain phytoplankton in the diet (Budge & Parrish 1998, Dalsgaard et al. 2003). Branched (iso and anteiso, denoted by *i*- and *a*-, respectively) and odd-numbered carbon chains have been applied as a biomarker for bacterial FAs (BAFAs; Budge & Parrish 1998). Specific FA ratios have been calculated to identify the importance of herbivory (e.g. $\Sigma\omega 3/\Sigma\omega 6$; Sargent & Falk-Petersen 1981) or carnivory and, in some locations, the dominance of dinoflagellates over diatoms (22:6 ω 3/20:5 ω 3; Parrish et al. 2000, Dalsgaard et al. 2003). In pyrosomes, some individual FAs have been applied as markers to identify dinoflagellates (e.g. 22:6 ω 3, 18:5 ω 3) or prymnesiophytes (18:1 ω 9, 18:4 ω 3; Perissinotto et al. 2007). However, relatively little is known about pyrosome FA or lipid metabolism, which complicates the interpretation of these FA biomarkers. The few existing studies on pyrosome FAs were conducted in the Southern and Indian Oceans (Mayzaud et al. 2007, Perissinotto et al. 2007, Richoux 2011). Researchers have hypothesized that at cooler temperatures (e.g. minimum of 11°C), pyrosome FAs indicate a more herbivorous diet, while at warmer temperatures (maximum of 20°C), FAs reflect carnivorous feeding (Richoux 2011).

Stable isotope (SI) analysis is a long-established tool for examining trophic relationships (Boecklen et al. 2011) in aquatic food webs. The isotopic composition of consumers is assumed to be similar to their diet, with predictable trophic fractionation; carbon ratios remain stable (<1‰) during trophic transfer while nitrogen values become enriched by around 3.4‰ from prey to predator (Peterson & Fry 1987), although this enrichment can vary between 2 and 4‰ (McCutchan et al. 2003). Accordingly, a consumer's ^{13}C isotope ratio is applied to identify reliance on different primary producers, whereas ^{15}N is used to estimate the consumer's trophic position relative to other consumers and base production. Previous SI analyses of pyrosomes have indicated that they occupy a unique position in the pelagic food web (Richoux & Froneman 2009, Décima et al. 2019). For species with difficult to observe feeding ecology, there is particular value in using a combined approach, which includes FAs and isotopes to generate hypotheses about trophic relationships (Pitt et al. 2008).

Due to the limited understanding of pyrosome abundance, distribution, and nutritional condition in the NCC, one cannot predict if or how their continued presence may alter food web dynamics through removal of phytoplankton biomass (Brodeur et al. 2017). To address these knowledge gaps, 2 primary hypotheses were addressed in the present study: (1)

changes in abiotic factors (e.g. temperature, salinity, fluorescence) would be associated with increased pyrosome abundance, and with increases in pyrosome abundance during blooms, pyrosomes would compete with other planktivorous organisms; and (2) pyrosome distribution would reflect potential differences in diet and nutritional condition. To address the first hypothesis, a generalized additive model (GAM) was used to identify relationships between *in situ* environmental variables (temperature, salinity, fluorescence) and the distribution and abundance patterns of pyrosomes in the NCC (42–49° N) during spring 2017. To assess whether pyrosome diet and condition is altered by distribution, FA profiles and dietary biomarkers were characterized and identified for pyrosomes collected in spring and summer 2017. We used FA biomarkers from the collected pyrosomes to compare spatial differences in pyrosome nutritive condition in the NCC in spring (May, on- and off-shelf) and summer (August) 2017. Finally, bulk SI analysis of carbon and nitrogen was used to examine spatial variation in potential food sources and trophic level of pyrosomes in the NCC.

2. MATERIALS AND METHODS

2.1. Field sampling

Pyrosomes were collected opportunistically during 2 research cruises in May and August 2017. The first cruise was a 10 d NCC ecosystem survey aboard the NOAA ship 'Bell M. Shimada', 14–24 May 2017 from Bodega Bay, CA (38° N) to Cape Meares, OR (45.5° N; see Fig. 1). Sampling at each station included net sampling for zooplankton using a vertically towed ring net (0.5 m diameter, 202 μm mesh; wire speed: 30 m min^{-1}) and an obliquely towed bongo net (0.6 m diameter, 0.5 mm mesh; ship speed: 1.5 knots; wire speed: 30 m min^{-1}). Nets were equipped with calibrated flow meters mounted in the net mouth and towed to maximum depth of 100 m, or 5 m off the bottom at shallower stations. Pyrosomes collected in the vertical ring and oblique bongo net tows were counted and measured, and a sub-sample of up to 5 individuals was rinsed with filtered seawater and placed in a -80°C freezer for subsequent FA and SI analysis. Pyrosomes zooids may not have had time to fully evacuate their guts prior to freezing, which may have influenced FA and SI results. However, due to the low volume of ingested material to total volume of pyrosome tissue analyzed, interpretation of the results was likely not affected. Pyrosome catch was

standardized to the volume sampled (m^3) for both sampling gears. CTD casts for *in situ* environmental conditions (SST, salinity, DO, and chlorophyll *a* [chl *a*] with depth) were also collected.

Pyrosomes were collected on a second research cruise aboard the 'Shimada' from 11–26 August 2017 during a NOAA Fishery Survey from Newport, OR (44.65°N, 124.5°W), to the north end of Vancouver Island (50.9°N, 129.7°W). Pyrosomes were collected, measured, and frozen for biochemical analyses from large midwater trawls (Aleutian wing trawl with 875 m^2 mouth opening) and a Methot trawl (5 m^2 mouth opening with 1 × 2 mm mesh). Pyrosome sampling on the August cruise was non-quantitative: pyrosome abundance was not standardized to volume sampled. For this reason, the FA and SI analyses presented (see Table 1) focus on the May 2017 cruise. Though there are limitations with the sampling scheme owing to differences in gear types and lack of replication, abundances for the May 2017 cruise are reported for 2 reasons: (1) the data can be put into context of other recent reports of pyrosome abundance (Brodeur et al. 2019a, Miller et al. 2019) and (2) the relative spatial abundance patterns are of interest (e.g. more pyrosomes offshore than onshore in May 2017).

2.2. FA analysis

Immediately following collection, pyrosomes were measured and stored individually in a -80°C freezer on board the research vessel and then transferred to a -20°C freezer in the lab for 3 mo until processing. To prepare samples ($n_{\text{May}} = 69$, $n_{\text{August}} = 22$) for lipid and FA extraction, they were first freeze-dried, then ground to a powder using a marble mortar and pestle. Material was weighed to 40 ± 0.3 mg and placed in a 10 ml centrifuge tube, then mixed with a chloroform:methanol (2:1) solution. Nondecanoic acid (C19) was added as an internal standard due to its low concentration in marine samples. After adding the C19 standard, the sample was flushed with nitrogen, sonicated in an ice-water bath, and centrifuged for 5 min at 3000 rpm, 4°C . The chloroform/organic layer containing the dissolved lipids was then transferred to a new 8 ml scintillation vial. This transfer process was repeated twice before evaporating the organic layer under nitrogen down to 1.5 ml. A 1 ml aliquot of the organic layer was then removed for transesterification, and the remaining 0.5 ml of material was preserved at -20°C for gravimetry (Taipale et al. 2016, Schram et al. 2018).

To begin the transesterification of FA, 1 ml toluene and 2 ml 1 % sulfuric acid:methanol solution was added to the lipid extract. Samples were then heated in a water bath for 90 min at 90°C . After transesterification, samples were left to cool to room temperature before adding 2 ml hexane and 1.5 ml sodium bicarbonate. The sample was vortexed for 10 s and centrifuged for 2 min at 1500 rpm at 4°C . The FA methyl esters (FAMES) in the upper layer were isolated and evaporated under nitrogen. FAMES were re-suspended for a second time by adding 1.5 ml hexane, evaporated to dryness and then transferred to a gas chromatograph vial for analysis (Taipale et al. 2016, Schram et al. 2018). FAs were processed for analysis through a GC-MS (Model QP2020, Shimadzu; Schram et al. 2018).

2.3. SI analysis

In the laboratory, frozen *Pyrosoma atlanticum* colonies ($n_{\text{May}} = 51$) were thawed and rinsed gently with deionized water. Colonies were transferred to individual weighing boats and placed in a drying oven at $55\text{--}60^\circ\text{C}$ for 48 h. Optimal weight ranges, based on $\delta^{13}\text{C}:\delta^{15}\text{N}$ values, were determined at the Oregon State University Stable Isotope Laboratory in Corvallis, OR, USA. Nitrogen and carbon isotope compositions were analyzed by continuous-flow isotope using a Carlo Erba elemental analyzer connected to a Thermo DeltaPlus ratio mass spectrometer. Carbon isotope data were calibrated against Vienna Pee Dee Belemnite (VPDB) using the international standard USGS40 and an internal lab standard SIL Sucrose. USGS40 and IAEA-N2 were used as standards for nitrogen. An international standard, caffeine, was used as check standard against VPDB and N_2 . Typical standard error is ± 0.1 for $\delta^{13}\text{C}$ and ± 0.2 for $\delta^{15}\text{N}$. Isotopic ratios are expressed as delta (δ) values in parts per thousand relative to international measurement standards.

2.4. Statistical analysis

The relationship between pyrosome abundance and distribution and environmental predictor variables in May 2017 (SST, salinity, fluorescence, and DO) was assessed using a GAM, the non-parametric equivalent of a general linear model, with the 'mgcv' package in R v.3.6.1 (Wood 2017, R Core Team 2019). Abundance and distribution graphics were generated in MATLAB. FA comparisons were per-

formed using routines in PRIMER v.6.1.13 (Clarke & Gorley 2006) with the PERMANOVA+ v.1.0.3 add-on (Anderson et al. 2008). Analysis of FA data included a non-metric multidimensional scaling (nMDS, using 'metaMDS' in the 'vegan' package in R; Oksanen et al. 2019) technique to visualize the similarities and differences between FA proportions and temporal (cruise month) and spatial factors (cruise month, distance off shelf, latitude); vectors represent those FAs contributing to $\geq 1\%$ of identified FAs. For distance-off-shelf comparisons, pyrosomes that had been collected during the May cruise at stations with a bottom depth < 250 m were considered to have been collected on the shelf, and pyrosomes collected from stations with a bottom depth of ≥ 250 m as off-shelf. Latitudes at which samples were collected in May were grouped into bins for distributional analysis (north: north of 44° N; middle: $43\text{--}44^\circ$ N; south: south of 43° N). Differences in FA proportions were tested using a 1-way permutational multivariate analyses of variance (PERMANOVA; $\alpha < 0.05$, 22 FAs; Table 1) comparing cruises (analysis includes samples collected on May and August cruises). Additional 1-way PERMANOVAs were used to analyze May cruise data to compare distance off-shelf, latitude, and size (divided into 3 size bins representing small: 5–10 cm; medium: 11–17 cm; and large: ≥ 18 cm). Comparisons of the May and August 2017 cruises were complicated by the different sample sizes and lack of spatial or temporal overlap. Cruise comparisons were made using nMDS and PERMANOVA to assess the appropriateness of combining data sets. Despite the inability of the present study to make comprehensive comparisons with the May data, the August data were included as a reference.

Univariate FA comparisons (parametric: *t*-test, ANOVA; nonparametric: Welch's *t*-test) were used to analyze the effect of distance offshore, latitude, and size of May pyrosomes (Tables 1 & S1 in the Supple-

ment at www.int-res.com/articles/suppl/m651p097_supp.pdf) on summary biomarkers after testing for normality (Shapiro-Wilk test) and homoscedasticity (Bartlett test); if data failed either test, nonparametric equivalents for *t*-test (Welch's *t*-test) and 1-way ANOVA (Welch's ANOVA) were used because they are more robust when groups are heterogenous regardless of data transformation (Lix et al. 1996). Summary biomarkers applied in previous studies were employed to evaluate pyrosome diets, including the ratio of 18:1 ω 9:18:1 ω 7 (an indicator of relative carnivory), BAFAs (branched and odd chain FAs), 16:1 ω 7 (e.g. diatoms), 18:2 ω 6 (e.g. chlorophytes), 18:4 ω 3 (e.g. prymnesiophytes), and 22:6 ω 3 (e.g. dinoflagellates) (Mayzaud et al. 2007, Richoux 2011). These biomarkers are prevalent for these sources in the NCC pelagic research context. Comparisons of univariate FA biomarkers were run in R (R Core Team 2019).

Statistical comparisons of SI ratios of C and N were made among the same latitudinal, onshore–offshore, and size-related bins as the FA data using 1-way ANOVA, or a Kruskal-Wallis 1-way ANOVA on ranks when the assumption of normality or equal variances was not met, followed by pairwise multiple comparison procedures (Student-Newman-Keuls method) to determine which levels were significantly different.

3. RESULTS

3.1. Pyrosome abundance, distribution, and environmental variables

Pyrosomes collected during the May 2017 research cruise in the NCC reached densities up to 5 colonies m^{-3} (Fig. 1). Mean pyrosome length was 13.6 cm (range: 6–78 cm) in May off northern California and Oregon and 11.5 cm (range 2–24 cm) in August off

Table 1. Statistical comparisons used for pyrosome analysis, including sample sizes for distance (on- or off-shelf), latitude (north: north of 44° N; middle: $43\text{--}44^\circ$ N; south: south of 43° N), and size (small: 5–10 cm; medium: 11–17 cm; large: ≥ 18 cm) comparisons. FA: fatty acid; SI: stable isotope; nMDS: non-metric multidimensional scaling

Comparisons	Factors	Sample size	Statistical comparisons
Cruise (May and Aug)	FA	May: 69, Aug: 22	nMDS, 1-way PERMANOVA
Distance (May)	FA	On: 17, Off: 52	nMDS, 1-way PERMANOVA, <i>t</i> -test, Welch's <i>t</i> -test
Latitude (May)	FA	North: 35, Middle: 11, South: 23	nMDS, 1-way PERMANOVA, ANOVA, Welch's ANOVA
Size (May)	FA	Small: 10, Medium: 37, Large: 22	nMDS, 1-way PERMANOVA, ANOVA, Welch's ANOVA
Distance (May)	SI	On: 29, Off: 7	nMDS, Mann-Whitney
Latitude (May)	SI	North: 29, Middle: 7, South: 12	nMDS, ANOVA/Kruskal-Wallis
Size (May)	SI	Small: 16, Medium: 27, Large: 5	nMDS, ANOVA/Kruskal-Wallis

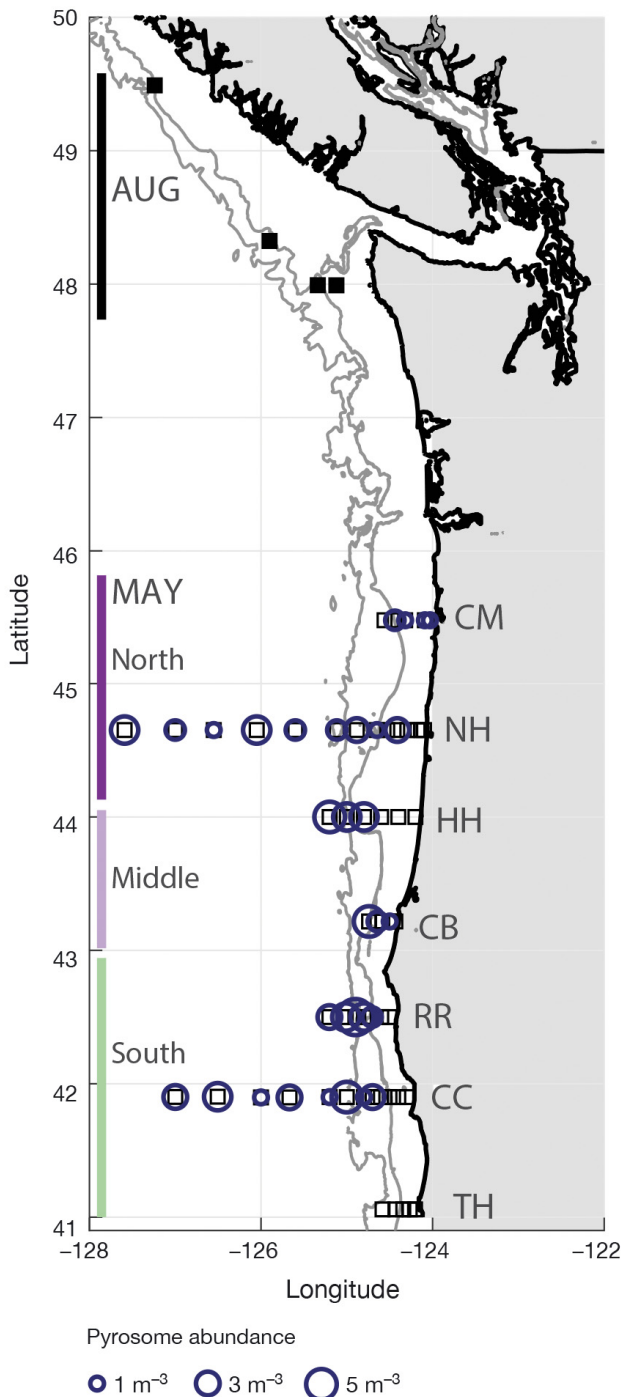


Fig. 1. Sampling locations from May 2017 (open squares) and August 2017 (filled squares). Bubble size corresponds to abundance of pyrosomes (colonies m^{-3}) at a given sampling site during the May 2017 cruise. Abundance was not quantified during the August 2017 cruise. Vertical lines highlight stations included in May latitude comparisons (north, middle, and south). Light gray lines: 250 (used to delineate on-shore vs. offshore groupings) and 1000 m contours. Labels indicate traditional sampling lines: TH: Trinidad Head; CC: Crescent City; RR: Rogue River; CB: Cape Blanco; HH: Heceta Head; NH: Newport Hydrographic; CM: Cape Meares

Washington and British Columbia. Pyrosomes were distributed near shore and in shelf regions. The highest catches of pyrosomes were off the Rogue River (RR), Heceta Head (HH), and Newport (NH), Oregon in May (5 colonies m^{-3} ; Fig. 1). The GAM identified SST and surface salinity as significant variables ($p < 0.05$) related to pyrosome densities in May 2017. Pyrosome aggregations were concentrated at locations with warmer SST ($12\text{--}14^\circ\text{C}$), moderate salinity (31–33 PSU), and lower fluorescence at 5 m depth ($<2\text{ mg l}^{-1}$; Table 2, Fig. 2).

3.2. FA analysis

Of the 46 FAs identified, 22 contributed a mean of $\geq 0.5\%$ in the pyrosomes collected (Tables S2 & S3). FAs from May and August cruises (Fig. 3A) were significantly different (PERMANOVA, Pseudo- $F = 19.08$, $df = 1$, $p = 0.001$; Fig. 3A). The FAs that contributed to $\geq 1\%$ of identified FAs included BAFAs (branched and odd-number carbon chain lengths), dinoflagellates (22:6 ω 3), and prymnesiophytes (18:4 ω 3), with the largest separation between samples collected during the May cruise being driven by BAFAs (19:1; Fig. 3A). The FAs of pyrosomes collected on both cruises did not differ with respect to distance from shore (on- vs. off-shelf; PERMANOVA, Pseudo- $F = 2.99$, $p = 0.03$) or size (PERMANOVA, Pseudo- $F = 1.72$, $df = 2$, $p = 0.08$). For the May samples (Fig. 3B), the FA profiles of pyrosomes differed by distance (on-shelf: bottom depth $<250\text{ m}$, off-shelf: bottom depth $\geq 250\text{ m}$; PERMANOVA, Pseudo- $F = 2.99$, $p = 0.03$) and latitude (north, middle, south; PERMANOVA, Pseudo- $F = 4.68$, $p < 0.001$; Fig. 3C).

There were fewer significant differences in summary biomarkers for comparisons of pyrosomes col-

Table 2. Generalized additive model results showing the relationship between May pyrosome abundance and *in situ* environmental variables including sea surface temperature (SST), surface salinity, and fluorescence. (*) indicates significance ($p \leq 0.05$) of the covariate along with the associated p-value. Relationships between the covariates and pyrosome abundance are shown as increasing or not significant (NS)

Covariates related to <i>Pyrosoma atlanticum</i> abundance (km^{-2})	p	Relationship
SST ($^\circ\text{C}$; 5 m)	$<0.001^*$	Increasing
Surface salinity (PSU)	$<0.05^*$	Increasing
Fluorescence	>0.05	NS

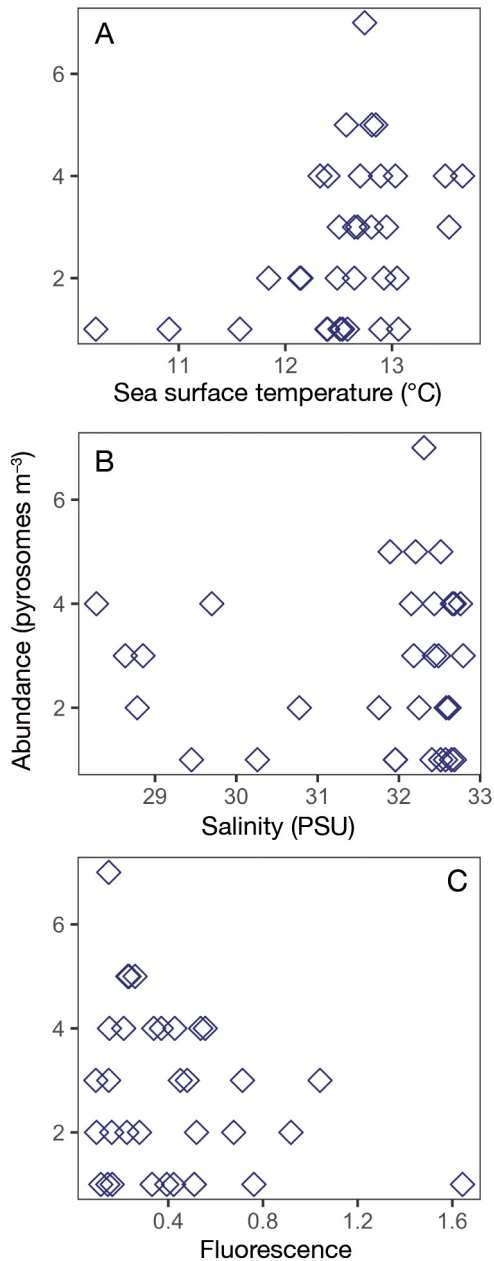


Fig. 2. May 2017 pyrosome abundance plotted against *in situ* environmental parameters at 5 m from CTD casts: (A) sea surface temperature, (B) salinity, and (C) fluorescence. Relationship between pyrosome abundance and environmental parameters was examined with a generalized additive model (Table 2)

lected on/off the shelf than for biomarkers from pyrosomes affiliated with distance from shore (Fig. 4, Table 3). The FA 18:4 ω 3 (an indicator of prymnesiophytes) was higher for pyrosomes collected off-shelf (mean \pm SD: 3.59 ± 1.13) than on (3.16 ± 1.23 ; Fig. 4A, Table 3). The highest levels of 18:4 ω 3 were observed

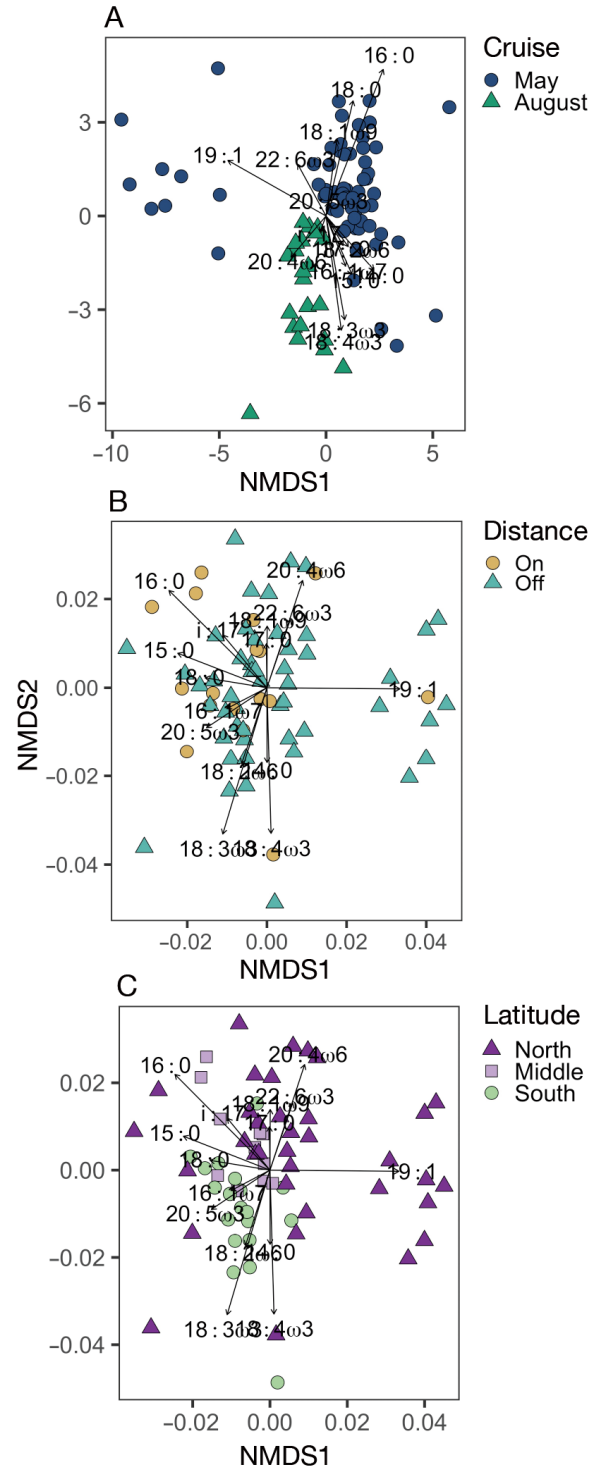


Fig. 3. Non-metric multidimensional scaling (nMDS) plots of Euclidean distances between the proportions of 46 fatty acids (FAs) in pyrosomes collected on research cruises (A) in May and August ($n = 69$ and 22 , respectively), (B) on the May cruise only, by distance offshore (on- or off-shelf; $n = 17$ and 52 , respectively), and (C) May data grouped by pre-determined latitude bins (north: north of 44° N; middle: 43 – 44° N; south: south of 43° N; $n = 35$, 11 , and 23 , respectively) with vector overlays of the FAs that contributed $\geq 5\%$ of FAs identified. Each symbol represents one sample

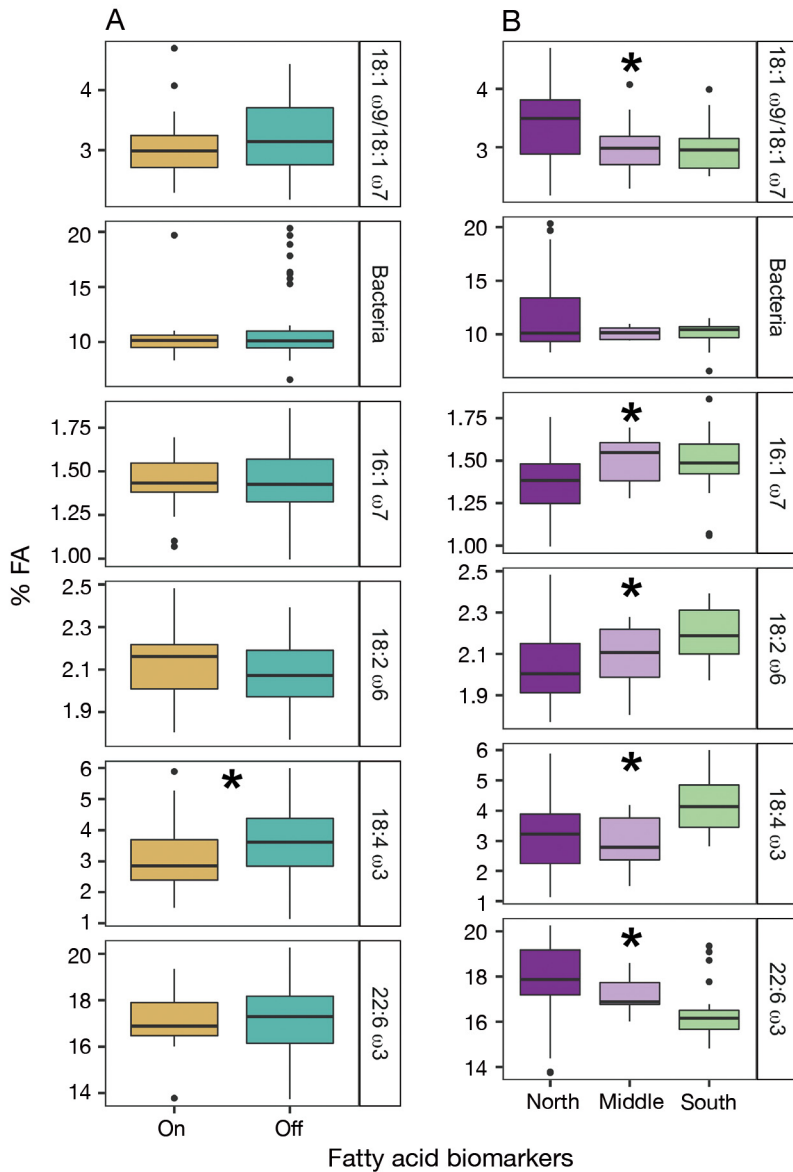


Fig. 4. Commonly used fatty acid (FA) biomarker indices including ratio of 18:1 ω 9/18:1 ω 7 (potential indicator of relative carnivory) and bacteria (branched and odd chain FAs) and FAs previously used as biomarkers in pyrosomes including 16:1 ω 7 (e.g. diatoms), 18:2 ω 6 (e.g. chlorophytes), 18:4 ω 3 (e.g. prymnesiophytes), and 22:6 ω 3 (e.g. dinoflagellates) for May collections comparing (A) distance (on-shelf: depth < 250 m; off-shelf: depth \geq 250 m; n = 17 and 52, respectively) and (B) latitude (north: north of 44° N; middle: 43–44° N; south: south of 43° N; n = 35, 11, and 23, respectively). Solid horizontal lines: median; lower and upper box boundaries: 25th and 75th quartiles; whiskers: data range (no more than 1.5 \times the length of boxes); filled circles: outliers. Significant comparisons ($p \leq 0.05$) are denoted with (*)

in the south latitude bin (Fig. 4B, Table 3). In contrast, there were significant differences in the FA of pyrosomes collected across latitude for biomarkers for 'carnivory', diatoms, chlorophytes, prymnesiophytes, and dinoflagellates (Fig. 4B, Table 3). The most frequent differences were between pyrosomes

collected in the north and south latitude bins, with values of FA biomarkers for the northern pyrosomes being greater than FA biomarker values collected in the south. Large pyrosomes had a significantly greater ratio of 18:1 ω 9/18:1 ω 7 than the medium or small size classes (Table 3).

3.3. SI analysis

Values of $\delta^{13}\text{C}$ and $\delta^{15}\text{N}$ were compared for pyrosomes collected in May associated with distance offshore, latitude, and pyrosome length (Fig. 5, Table 4). Despite a large amount of overlap of pyrosomes collected across distance and latitude ranges (Fig. 5), the $\delta^{13}\text{C}$ and $\delta^{15}\text{N}$ of May collections were significantly different in pyrosomes collected offshore and across May cruise latitudes. The $\delta^{13}\text{C}$ values of pyrosomes collected in the north were significantly higher than either the middle (43–44° N) or the southern end of the sampling region (south of 43° N), while $\delta^{15}\text{N}$ was higher in the south than the north (Table 4). The $\delta^{13}\text{C}$ of pyrosomes collected onshore was significantly higher than pyrosomes collected offshore, whereas the $\delta^{15}\text{N}$ was significantly lower for shelf pyrosomes than those $\delta^{15}\text{N}$ values collected offshore (Table 4). These latter trends were also seen for the Newport Line only (data not shown). There were no differences in pyrosome $\delta^{13}\text{C}$ or $\delta^{15}\text{N}$ associated with colony length (Table 4).

4. DISCUSSION

Pyrosome feeding ecology has not been well studied in any part of their typical range and has not been investigated in the NCC. We found pyrosome abundance in May 2017 to be significantly associated with warmer surface water, moderate salinity, and lower fluorescence (Table 2). There were no differences in FA or SI biomarkers that were associated with colony size (Tables 3 & 4) but there were significant differ-

Table 3. Comparisons (2 sample *t*-test or 1-way ANOVA) of fatty acid biomarkers quantified in pyrosomes that were collected in May 2017 on ($n = 17$) and off ($n = 52$) the continental shelf (Distance), across latitude (Latitude; north: north of 44°N ; middle: $43\text{--}44^\circ\text{N}$; south: south of 43°N ; $n = 35, 11,$ and 23 , respectively), and size classes (small: $5\text{--}10\text{ cm}$; medium: $11\text{--}17\text{ cm}$; large: $\geq 18\text{ cm}$; $n = 10, 37,$ and 22 , respectively). Biomarkers are described in Section 2. Welch's *t*-tests or Welch's ANOVA were used to test for differences in data that failed tests for normality or homoscedasticity. NS: no significant differences for the main statistical test and/or pairwise comparisons; * $p \leq 0.05$

		Test	Statistic	df (num, denom)	p	Relationship
Distance	18:1 ω 9:18:1 ω 7	Welch's <i>t</i> -test	0.61	(1.00, 26.14)	0.44	NS
	Bacteria	Welch's <i>t</i> -test	0.44	(1.00, 33.167)	0.51	NS
	16:1 ω 7	<i>t</i> -test	1.76	85	0.08	NS
	18:2 ω 6	<i>t</i> -test	0.69	85	0.49	NS
	18:4 ω 3	<i>t</i> -test	2.34	85	0.02*	Aug > May
	22:6 ω 3	<i>t</i> -test	-0.86	85	0.39	NS
Latitude	18:1 ω 9:18:1 ω 7	Welch's ANOVA	4.82	(2.00, 28.007)	0.02*	North > south
	Bacteria	Welch's ANOVA	3.13	(2.00, 43.032)	0.054	NS
	16:1 ω 7	ANOVA	3.82	2	0.03*	South > north
	18:2 ω 6	ANOVA	7.85	2	0.001*	North > south
	18:4 ω 3	ANOVA	6.52	2	0.003*	South > north, middle
	22:6 ω 3	Welch's ANOVA	7.13	(2.00, 37.544)	0.002*	North > south
Size	18:1 ω 9:18:1 ω 7	Welch's ANOVA	6.67	(2.00, 24.602)	0.005*	Large > medium, small
	Bacteria	Welch's ANOVA	2.86	(2.00, 43.171)	0.07	NS
	16:1 ω 7	ANOVA	0.77	2	0.47	NS
	18:2 ω 6	ANOVA	0.51	2	0.61	NS
	18:4 ω 3	ANOVA	0.48	2	0.62	NS
	22:6 ω 3	ANOVA	1.75	2	0.18	NS

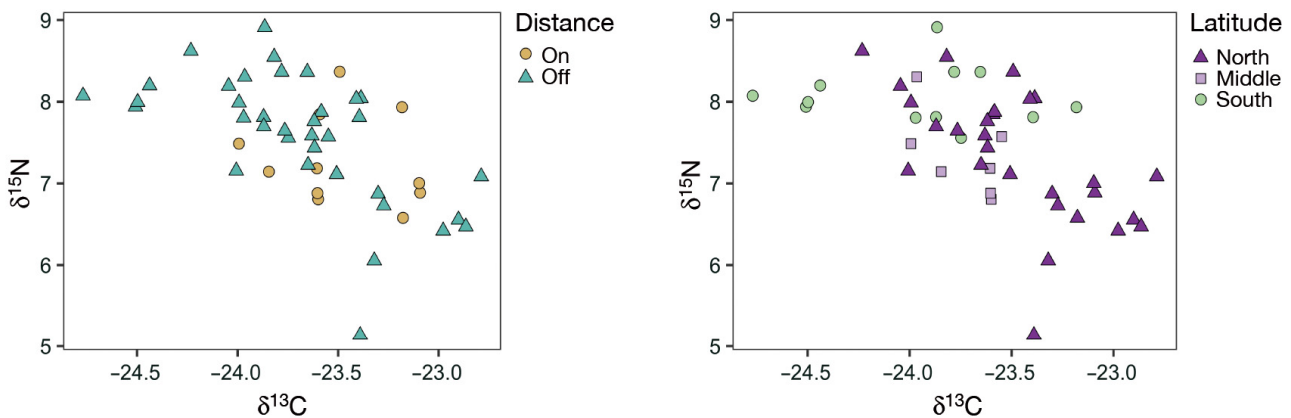


Fig. 5. Pyrosome stable isotope ($\delta^{15}\text{N}$ and $\delta^{13}\text{C}$) results from the May collection cruise associated with distance (on-shelf: depth $< 250\text{ m}$; off-shelf: depth $\geq 250\text{ m}$; $n = 29$ and 7 , respectively) and latitude (north: north of 44°N ; middle: $43\text{--}44^\circ\text{N}$; south: south of 43°N ; $n = 29, 7,$ and 12 , respectively)

ences in FA and SI based on distance offshore and latitude at which pyrosomes were collected (Figs. 3 & 4), suggesting these factors may have the most influence on pyrosome diet and condition in the NCC. Pyrosomes are one of the least studied pelagic tunicates (Perissinotto et al. 2007), and had not been recorded in the NCC off the Pacific Northwest coast prior to 2014 (Brodeur et al. 2017). Between 2016 and 2018, there were aggregations along the entire west

coast of the USA but the largest densities of pyrosomes were concentrated further north in the NCC ($42\text{--}48^\circ\text{N}$) during the spring and summer (Miller et al. 2019), leading to short- and potentially long-term changes to the pelagic marine ecosystem (Brodeur et al. 2017, Sutherland et al. 2018). This pyrosome range expansion offers a unique opportunity to characterize the potential ecosystem effects of a newly arrived consumer.

Table 4. One-way ANOVA or nonparametric Kruskal-Wallis or Mann-Whitney test results for comparisons of carbon and nitrogen stable isotope values of pyrosomes collected on the May 2017 cruise by distance offshore (on or off the shelf, n = 29 and 7, respectively), latitude (north: north of 44° N; middle: 43–44° N; south: south of 43° N; n = 29, 7, and 12, respectively), and size (small: 5–10 cm; medium: 11–17 cm; large: ≥18 cm; n = 16, 27, and 5, respectively). *p ≤ 0.05; NS: not significant

Factor	Isotope	Test	df	p	Relationship
Distance	C	Mann-Whitney	1	0.03*	Shelf > offshore
	N	Mann-Whitney	1	0.02*	Offshore > shelf
Latitude	C	Kruskal-Wallis	2	0.001*	North > middle, south
	N	ANOVA	2	0.008*	South > north
Size	C	ANOVA	2	0.66	NS
	N	Kruskal-Wallis	2	0.70	NS

During May 2017, the highest abundances of pyrosomes were in areas with warmer SSTs, between 12 and 15°C, which were above the typical average temperatures for NCC shelf waters during the summer. Sampling occurred during the warm water Blob, when regional SSTs were 2.5°C warmer than the long-term average and were associated with reduced nutrients and reduced phytoplankton productivity (Peterson et al. 2017). In addition to a relationship with temperature, results from GAM analysis of *in situ* environmental variables showed higher pyrosome abundance in moderate to high salinities (Fig. 2, Table 2). In August 2017, pyrosome aggregations were patchier and concentrated further onshore than the aggregations observed in May at more southern latitudes. Results did not indicate a significant relationship between pyrosome abundance and fluorescence measured near the surface (5 m depth; Table 2), which supports the idea that distributions correspond to temperature, salinity, and possibly food quality but not overall food availability.

Due to their efficient grazing on phytoplankton (Perissinotto et al. 2007), pyrosomes have the potential to impact phytoplankton assemblages where they form dense aggregations (Drits et al. 1992). Pyrosomes filter a variety of planktonic microorganisms, from diatoms and dinoflagellates larger than 10 µm (Perissinotto et al. 2007) to smaller diatoms and coccolithophores of 3–5 µm (Drits et al. 1992). Like other pelagic tunicates, pyrosomes may also be able to filter pico-phytoplankton and bacteria-plankton at the submicron scale (Sutherland 2010, Conley et al. 2018), and recent work has shown that appendicularians (Dadon-Pilosof et al. 2017) and salps (Dadon-Pilosof et al. 2019) can select prey independent of prey size. In salps, smaller picoeukaryotes were retained at higher retention efficiency

than larger nanoeukaryotes (Dadon-Pilosof et al. 2019). A broad prey size range with preference for smaller cells may allow pyrosomes to thrive in relatively low productivity zones. Weaker upwelling periods may favor pyrosomes in the NCC due to warmer waters and lower nutrients, conditions which are similar to tropical regions where pyrosomes have typically been concentrated.

The base of the NCC food web is characterized by seasonal and spatial variability in cyanobacteria and phytoplankton communities. During upwelling events, the shelf is dominated by

large diatoms, whereas during non-upwelling, diatom and dinoflagellate diversity and abundance are low (Du & Peterson 2018). *Synechococcus* and photosynthetic picoeukaryotes have been shown to be low in abundance on the shelf off the Oregon coast but dominant offshore where chlorophyll concentrations are low (Sherr et al. 2005). During warm anomalies in the NCC, such as during the sampling period, diatom abundance and diversity are low, whereas dinoflagellate abundance and diversity are high (Du & Peterson 2018). Considering the different community composition on and off the shelf, pyrosomes, which feed at a low trophic level, might be expected to reflect these spatial differences in phytoplankton. Surprisingly, the analyses reflected little if any differences in onshore vs. offshore samples; instead, most differences in biomarkers (especially FAs) were based on latitude (Tables 3 & 4). During the sampling period, latitudinal gradients in phytoplankton community composition off the Oregon coast may have been heterogeneous due to bathymetry or transient features such as river plumes (Kudela et al. 2008).

While there are published values of pyrosome clearance rates (Perissinotto et al. 2007, Conley et al. 2018), less is known about their diet composition, particularly in the NCC where they have not previously been observed. Informative diet FA biomarkers in pyrosomes differed across latitude for 18:1ω9/18:1ω7 and 22:6ω3 (carnivory and dinoflagellates, respectively; greatest in the north), 16:1ω7 (diatoms; greatest in the middle and south), as well as 18:2ω6 and 18:4ω3 (chlorophytes and prymnesiophytes, respectively; greatest in the south). Relative to distance comparisons, latitude differentiated pyrosome diet more than distance offshore, for which the only difference was for 18:4ω3 (greater offshore; Fig. 4). The relative carnivory index utilized here (ratio of

18:1 ω 9/18:1 ω 7) (Fig. 4B) was at a slightly higher level in the north latitudes in May than levels previously reported in zooplankton inhabiting surface seawater with temperatures greater than 11°C (Richoux 2011). The ratios of 18:1 ω 9/18:1 ω 7 for the middle and south latitudes of the present study are comparable to levels previously reported (Richoux 2011). FA analysis of *Pyrosoma atlanticum* in the south Indian Ocean pointed to a phytoplankton-based diet of diatoms (20:5 ω 3), dinoflagellates (22:6 ω 3), prymnesiophytes, coccolithophores (18:1 ω 9), and chlorophytes (18:3 ω 3) (Perissinotto et al. 2007).

FA profiles of *P. atlanticum* collected from the Southern Ocean showed the presence of 18:2 ω 6, a biomarker for chlorophytes or cyanobacteria (Richoux 2011). In Southern Ocean pyrosomes, 18:2 ω 6 differed from north to south and may have resulted from relative differences in 18:2 ω 6 in particulate organic material (Richoux 2011). We report similar levels of this chlorophyte/cyanobacteria marker, but these levels did not differ with distance offshore (on/off-shelf) or size (Table 3). BAFAs across samples that were similar to those levels previously reported for pyrosomes were observed (Perissinotto et al. 2007, Richoux 2011). August samples had higher levels of BAFAs than May samples (Fig. 4A). The most abundant FA was docosahexanoic acid (DHA; 22:6 ω 3) which, in pelagic systems, is a reasonable biomarker for dinoflagellates. Although there were slight differences between FA proportions by latitude, they were not statistically significant, suggesting that pyrosomes exhibit similar feeding habits in spring and later summer and over a broad latitudinal range (Fig. 3B, Table 3).

Based upon the mean $\delta^{15}\text{N}$ values (7.2 and 7.5 from shelf and offshore collections, respectively), *P. atlanticum* appears to feed at a relatively low trophic level compared to other zooplankton groups in the NCC region. For example, (Miller et al. 2010) reported that other crustacean zooplankton such as copepods, decapod larvae, and euphausiids had mean $\delta^{15}\text{N}$ values between 9.1 and 10.1‰ for the same general region in summer. Miller et al. (2010) also noted that the particulate organic matter (POM) baseline was between 5.7 and 6.5‰ for the slope and shelf, respectively. Although baseline POM isotopes were not measured in the present study, if similar POM values to the Miller et al. (2010) study were assumed, pyrosomes would represent a trophic position of around 1.5, compared to around 2.0 for most crustacean zooplankton in this region (Miller et al. 2010). However, as Décima et al. (2013) showed off Southern California, there can be a substantial (~2‰)

enrichment of baseline ^{15}N values during warm and low productivity years so the exact trophic position of pyrosomes in the present study is uncertain. In another study from the Subtropical Convergence Zone off South Africa, Richoux & Froneman (2009) found similar (mean 6.8‰) $\delta^{15}\text{N}$ values north of the convergence zone (nutrient-poor Indian Ocean waters) but far lower (2.1‰) values south of the zone in Southern Ocean waters. Similarly, Décima et al. (2019) reported that another pyrosome, *Pyrostremma spinosum*, from the Eastern Tropical Pacific had extremely low (mean $\delta^{15}\text{N}$ values of 4.5–5.1‰), which were well below other zooplankton groups and just above the POM baseline. In contrast, Gauns et al. (2015) reported $\delta^{15}\text{N}$ values of 7.43‰ for this same species in the Arabian Sea, almost identical to the offshore levels observed. Thus, it is challenging to consider pelagic tunicates as surrogates for baseline production in most ecosystems without complete knowledge of the phytoplankton community available to them. Indeed, Pakhomov et al. (2019) suggested instead that they may represent part of the microbial food web.

Many primary producers exhibit distinctive $\delta^{13}\text{C}$ signatures in different marine habitats, which may make potential carbon sources easier to distinguish. For the NCC, Miller et al. (2008) reported a decreasing trend in $\delta^{13}\text{C}$ with distance offshore, with significantly lower values off than on the shelf. Similar results are reported with the offshore values observed in the present study (mean: -23.75‰) being significantly lower than those values collected on the shelf (-23.54‰), suggesting some incorporation of more nearshore carbon into the pyrosome tissues. However, the shelf vs. slope ^{13}C differences reported by Miller et al. (2008) were higher for both POM ($\Delta 2.47\%$) and copepods ($\Delta 1-3\%$) than the ^{13}C differences for the pyrosomes reported here. The Miller et al. (2008) study took place during 2000 and 2002, both relatively strong upwelling years with high productivity on the shelf compared to 2017. Since these authors found a strong relationship between productivity (measured as chl *a*) and $\delta^{13}\text{C}$, this relationship may explain the higher overall $\delta^{13}\text{C}$ values as well as the greater cross-shelf differences. The residence time of *P. atlanticum* on the shelf is not known, and pyrosomes may have undertaken much of their food assimilation in offshore waters and before being transported onto the shelf prior to capture. Another factor confounding these results is that latitudinal differences in $\delta^{13}\text{C}$ (higher values to the north) were also observed, but there were significant differences when applying only the Newport Line data, which had the greatest cross-shelf rep-

resentation (Fig. 1). Thus, the location of capture may influence the relative trophic position and source production for *P. atlanticum* in the present study. Whole colonies were analyzed for isotope samples, and although no size-related trends were found in either isotope, there may be isotopic differences among the different zooids depending on their age and where they fed during their development. Like many other gelatinous zooplankton (see Pitt et al. 2008), information on turnover rates of C is lacking, which limits the ability to determine where isotopic signatures originate; however, based on this analysis, the population off Oregon likely came from a source farther offshore and south of the study area.

The northward expansion of *P. atlanticum* into the NCC may not be a temporary phenomenon and thus could lead to long-term changes in the marine pelagic food web (Sutherland et al. 2018). The biomass of *P. atlanticum* was extremely high off Oregon during the spring and summer of 2017 and again in 2018 before declining in this region but still maintaining high biomass off California in 2019 following the cessation of the marine heatwave (Miller et al. 2019). As ocean temperatures continue to rise globally, new marine heatwaves will probably develop and become more intense in the North Pacific (Oliver et al. 2019), which will provide suitable habitat for warm-water invaders such as *P. atlanticum* to become established in this temperate ecosystem.

The dense *P. atlanticum* aggregations in this study (up to 5 colonies m⁻³ at some locations) and high clearance rates may allow them to impact phytoplankton assemblages and alter energy transfer. The biomarker analysis in the present study suggests that pyrosomes feed on a broad range of planktonic microorganisms and that the highest proportions were markers for essential FAs including eicosapentaenoic acid and DHA. Although *P. atlanticum* appears to feed at a lower trophic level than many of the crustacean plankton such as copepods and euphausiids that normally have dominated the NCC pelagic food web, we do not know how much the removal of these microorganisms affects other components of the ecosystem. The biomasses of both copepods (Peterson et al. 2017) and euphausiids (Brodeur et al. 2019a, authors' unpubl. data in 2017) were orders of magnitude lower during the marine heatwave compared with normal years on the shelf off Oregon, but it is unknown whether this shift in available prey is an indirect effect of food limitation due to competition from the extremely high pyrosome biomass that year. More research into pyrosome feeding ecology is needed to better understand

their trophic niche and implications for the pelagic food web should they become established in temperate ocean regions. Similar to other thaliaceans, the role of pyrosomes as consumers and prey sources are underappreciated (Henschke et al. 2019). Although numerous fish taxa and even marine mammals were shown to be feeding on pyrosomes during the 2017 bloom (Brodeur et al. 2019b), their contribution to the pelagic food web is likely much lower than most crustacean zooplankton. Consequently, much of the biomass represented in this bloom may have settled to the bottom, where pyrosome tissues decomposed or became food for the benthos, as documented in the NCC and other ecosystems (Lebrato & Jones 2009, Archer et al. 2018). As pyrosomes continue to be a dominant presence in the California Current, additional research into the environmental drivers causing their range expansion will add clarity to their role in this productive pelagic ecosystem.

Acknowledgements. We thank the officers and crew of the R/V 'Shimada' for assistance in the at-sea sampling of pyrosomes. Jennifer Fisher and Sam Zeman were helpful in collecting and measuring the pyrosomes at sea. Jennifer McKay at the OSU Stable Isotope lab assisted with the isotope measurements. We thank Dr. Todd Miller (NOAA Alaska Fisheries Science Center), handling editor Dr. Marsh Youngbluth, and 3 anonymous reviewers for their helpful comments on an earlier version of the manuscript. We acknowledge the support of Oregon Sea Grant (R/ECO-30-PD to K. Sutherland and A. W. E. Galloway). We also acknowledge the NOAA Fisheries Northwest Fisheries Science Center for providing ship, logistic, and salary support.

LITERATURE CITED

- ✦ Allredge AL, Madin LP (1982) Pelagic tunicates: unique herbivores in the marine plankton. *Bioscience* 32: 655–663
- Anderson M, Gorley RN, Clarke RK (2008) PERMANOVA+ for PRIMER: guide to software and statistical methods. PRIMER-E, Plymouth
- ✦ Archer SK, Kahn AS, Leys SP, Norgard T, Girard F, Du Preez C, Dunham A (2018) Pyrosome consumption by benthic organisms during blooms in the northeast Pacific and Gulf of Mexico. *Ecology* 99:981–984
- ✦ Boecklen WJ, Yarnes CT, Cook BA, James AC (2011) On the use of stable isotopes in trophic ecology. *Annu Rev Ecol Evol Syst* 42:411–440
- Bograd SJ, Schroeder I, Sarkar N, Qiu X, Sydeman WJ, Schwing FB (2009) Phenology of coastal upwelling in the California Current. *Geophys Res Lett* 36:L01602
- ✦ Bond NA, Cronin MF, Freeland H, Mantua N (2015) Causes and impacts of the 2014 warm anomaly in the NE Pacific. *Geophys Res Lett* 42:3414–3420
- Brodeur R, Perry I, Boldt J, Flostrand L and others (2017) An unusual gelatinous plankton event in the NE Pacific: the great pyrosome bloom of 2017. *PICES Press* 26:22–27
- ✦ Brodeur RD, Auth TD, Phillips AJ (2019a) Major shifts in

- pelagic micronekton and macrozooplankton community structure in an upwelling ecosystem related to an unprecedented marine heatwave. *Front Mar Sci* 6:212
- Brodeur RD, Hunsicker ME, Hann A, Miller TW (2019b) Effects of warming ocean conditions on feeding ecology of small pelagic fishes in a coastal upwelling ecosystem: a shift to gelatinous food sources. *Mar Ecol Prog Ser* 617-618:149–163
- Brotz L, Cheung WWL, Kleisner K, Pakhomov E, Pauly D (2012) Increasing jellyfish populations: trends in large marine ecosystems. In: Purcell J, Mianzan H, Frost JR (eds) *Jellyfish blooms IV. Developments in hydrobiology*, Vol 220. Springer, Dordrecht, p 3–20
- Budge SM, Parrish CC (1998) Lipid biogeochemistry of plankton, settling matter and sediments in Trinity Bay, Newfoundland. II. Fatty acids. *Org Geochem* 29: 1547–1559
- Checkley DM, Barth JA (2009) Patterns and processes in the California Current System. *Prog Oceanogr* 83:49–64
- Clarke K, Gorley R (2006) *PRIMER v6: user manual*. PRIMER-E, Plymouth
- Conley KR, Lombard F, Sutherland KR (2018) Mammoth grazers on the ocean's minuteness: a review of selective feeding using mucous meshes. *Proc R Soc B* 285: 20180056
- Culkin F, Morris RJ (1970) The fatty acid composition of two marine filter-feeders in relation to a phytoplankton diet. *Deep Sea Res Oceanogr Abstr* 17:861–865
- Dadon-Pilosof A, Conley KR, Jacobi Y, Haber M and others (2017) Surface properties of SAR11 bacteria facilitate grazing avoidance. *Nat Microbiol* 2:1608–1615
- Dadon-Pilosof A, Lombard F, Genin A, Sutherland KR, Yahel G (2019) Prey taxonomy rather than size determines salp diets. *Limnol Oceanogr* 64:1996–2010
- Dalsgaard J, John MS, Kattner G, Müller-Navarra D, Hagen W (2003) Fatty acid trophic markers in the pelagic marine environment. *Adv Mar Biol* 46:225–340
- Décima M, Landry MR, Popp BN (2013) Environmental perturbation effects on baseline $\delta^{15}\text{N}$ values and zooplankton trophic flexibility in the southern California Current Ecosystem. *Limnol Oceanogr* 58:624–634
- Décima M, Stukel MR, López-López L, Landry MR (2019) The unique ecological role of pyrosomes in the Eastern Tropical Pacific. *Limnol Oceanogr* 64:728–743
- Di Lorenzo E, Mantua N (2016) Multi-year persistence of the 2014/15 North Pacific marine heatwave. *Nat Clim Chang* 6:1042–1047
- Drits AV, Arashkevich EG, Semenova TN (1992) *Pyrosoma atlanticum* (Tunicata, Thaliacea): grazing impact on phytoplankton standing stock and role in organic carbon flux. *J Plankton Res* 14:799–809
- Du X, Peterson WT (2018) Phytoplankton community structure in 2011–2013 compared to the extratropical warming event of 2014–2015. *Geophys Res Lett* 45:1534–1540
- Gauns M, Mochemadkar S, Pratihary A, Roy R, Naqvi SWA (2015) Biogeochemistry and ecology of *Pyrosoma spinosum* from the Central Arabian Sea. *Zool Stud* 54:3
- Godeaux J (1998) The relationships and systematics of the Thaliacea with keys for identification. In: Bone Q (ed) *The biology of pelagic tunicates*. Oxford University Press, Oxford, p 273–294
- Graham WM, Gelcich S, Robinson KL, Duarte CM and others (2014) Linking human well-being and jellyfish: ecosystem services, impacts, and societal responses. *Front Ecol Environ* 12:515–523
- Henschke N, Pakhomov EA, Kwong LE, Everett JD, Laiolo L, Coghlan AR, Suthers IM (2019) Large vertical migrations of *Pyrosoma atlanticum* play an important role in active carbon transport. *J Geophys Res Biogeosci* 124: 1056–1070
- Jacox MG, Hazen EL, Zaba KD, Rudnick DL, Edwards CA, Moore AM, Bograd SJ (2016) Impacts of the 2015–2016 El Niño on the California Current System: early assessment and comparison to past events. *Geophys Res Lett* 43:7072–7080
- Kelly JR, Scheibling RE (2012) Fatty acids as dietary tracers in benthic food webs. *Mar Ecol Prog Ser* 446:1–22
- Kudela RM, Banas NS, Barth JA, Frame ER and others (2008) New insights into the controls and mechanisms of plankton productivity in coastal upwelling waters of the Northern California Current system. *Oceanography* (Wash DC) 21:46–59
- Lebrato M, Jones DOB (2009) Mass deposition event of *Pyrosoma atlanticum* carcasses off Ivory Coast (West Africa). *Limnol Oceanogr* 54:1197–1209
- Lix LM, Keselman JC, Keselman HJ (1996) Consequences of assumption violations revisited: a quantitative review of alternatives to the one-way analysis of variance *F* test. *Rev Educ Res* 66:579–619
- Lynam CP, Hay SJ, Brierley AS (2004) Interannual variability in abundance of North Sea jellyfish and links to the North Atlantic Oscillation. *Limnol Oceanogr* 49:637–643
- Mayzaud P, Boutoute M, Perissinotto R, Nichols P (2007) Polar and neutral lipid composition in the pelagic tunicate *Pyrosoma atlanticum*. *Lipids* 42:647–657
- McCutchan JH, Lewis WM, Kendall C, McGrath CC (2003) Variation in trophic shift for stable isotope ratios of carbon, nitrogen, and sulfur. *Oikos* 102:378–390
- Miller TW, Brodeur RD, Rau GH (2008) Carbon stable isotopes reveal relative contribution of shelf-slope production to the Northern California Current pelagic community. *Limnol Oceanogr* 53:1493–1503
- Miller TW, Brodeur RD, Rau G, Omori K (2010) Prey dominance shapes trophic structure of the northern California Current pelagic food web: evidence from stable isotopes and diet analysis. *Mar Ecol Prog Ser* 420:15–26
- Miller RR, Santora JA, Auth TD, Sakuma KM, Wells BK, Field JC, Brodeur RD (2019) Distribution of pelagic thaliaceans, *Thetys vagina* and *Pyrosoma atlanticum*, during a period of mass occurrence within the California Current. *CalCOFI Rep* 60:94–108
- Oksanen J, Blanchet FG, Friendly M, Kindt R and others (2019) *vegan: community ecology package*. R package version 2.5.4
- Oliver EC, Donat MG, Burrows MT, Moore PJ and others (2018) Longer and more frequent marine heatwaves over the past century. *Nat Commun* 9:1324
- Oliver EC, Burrows MT, Donat MG, Sen Gupta A and others (2019) Projected marine heatwaves in the 21st century and the potential for ecological impact. *Front Mar Sci* 6: 734
- Pakhomov EA, Henschke N, Hunt BP, Stowasser G, Cherel Y (2019) Utility of salps as a baseline proxy for food web studies. *J Plankton Res* 41:3–11
- Parrish CC, Abrajano TA, Budge SM, Helleur RJ, Hudson ED, Pulchan K, Ramos C (2000) Lipid and phenolic biomarkers in marine ecosystems: analysis and applications. In: Wangersky PJ (ed) *Marine chemistry*. Springer, New York, NY, p 193–223
- Perissinotto R, Mayzaud P, Nichols PD, Labat JP (2007)

- Grazing by *Pyrosoma atlanticum* (Tunicata, Thaliacea) in the south Indian Ocean. *Mar Ecol Prog Ser* 330:1–11
- Peterson BJ, Fry B (1987) Stable isotopes in ecosystem studies. *Annu Rev Ecol Syst* 18:293–320
- Peterson WT, Fisher JL, Strub PT, Du X, Risien C, Peterson J, Shaw CT (2017) The pelagic ecosystem in the Northern California Current off Oregon during the 2014–2016 warm anomalies within the context of the past 20 years. *J Geophys Res Oceans* 122:7267–7290
- Pitt KA, Connolly RM, Meziane T (2008) Stable isotope and fatty acid tracers in energy and nutrient studies of jellyfish: a review. In: Pitt KA, Purcell JE (eds) *Jellyfish blooms: causes, consequences, and recent advances*. *Developments in hydrobiology*, Vol 206. Springer, Dordrecht, p 119–132
- Purcell JE, Uye S, Lo W (2007) Anthropogenic causes of jellyfish blooms and their direct consequences for humans: a review. *Mar Ecol Prog Ser* 350:153–174
- R Core Team (2019) R: a language and environment for statistical computing. R Foundation for Statistical Computing, Vienna
- Richoux NB (2011) Trophic ecology of zooplankton at a frontal transition zone: fatty acid signatures at the subtropical convergence, Southern Ocean. *J Plankton Res* 33:491–505
- Richoux NB, Froneman PW (2009) Plankton trophodynamics at the subtropical convergence, Southern Ocean. *J Plankton Res* 31:1059–1073
- Sargent JR, Falk-Petersen S (1981) Ecological investigations on the zooplankton community in Balsfjorden, Northern Norway: lipids and fatty acids in *Meganyctiphanes norvegica*, *Thysanoessa raschi* and *T. inermis* during mid-winter. *Mar Biol* 62:131–137
- Schram JB, Kobelt JN, Dethier MN, Galloway AW (2018) Trophic transfer of macroalgal fatty acids in two urchin species: digestion, egestion, and tissue building. *Front Ecol Evol* 6:83
- Sherr EB, Sherr BF, Wheeler PA (2005) Distribution of coccooid cyanobacteria and small eukaryotic phytoplankton in the upwelling ecosystem off the Oregon coast during 2001 and 2002. *Deep Sea Res II* 52:317–330
- Suchman CL, Brodeur RD, Daly EA, Emmett RL (2012) Large medusae in surface waters of the Northern California Current: variability in relation to environmental conditions. *Hydrobiologia* 690:113–125
- Sutherland KR (2010) Form, function and flow in the plankton: jet propulsion and filtration by pelagic tunicates. PhD thesis, Woods Hole Oceanographic Institution and Massachusetts Institute of Technology, Cambridge, MA
- Sutherland KR, Sorensen HL, Blondheim ON, Brodeur RD, Galloway AW (2018) Range expansion of tropical pyrosomes in the northeast Pacific Ocean. *Ecology* 99: 2397–2399
- Taipale SJ, Hiltunen M, Vuorio K, Peltomaa E (2016) Suitability of phytosterols alongside fatty acids as chemotaxonomic biomarkers for phytoplankton. *Front Plant Sci* 7:212
- Tilves U, Fuentes VL, Milisenda G, Parrish CC, Vizzini S, Sabatés A (2018) Trophic interactions of the jellyfish *Pelagia noctiluca* in the NW Mediterranean: evidence from stable isotope signatures and fatty acid composition. *Mar Ecol Prog Ser* 591:101–116
- Van Soest RWM (1981) A monograph of the order Pyrosomatida (Tunicata, Thaliacea). *J Plankton Res* 3:603–631
- Wood SN (2017) *Generalized additive models: an introduction with R*. CRC Press, Boca Raton, FL
- Zeman SM, Corrales-Ugalde M, Brodeur RD, Sutherland KR (2018) Trophic ecology of the neustonic cnidarian *Velevella velevella* in the Northern California Current during an extensive bloom year: insights from gut contents and stable isotope analysis. *Mar Biol* 165:150

Editorial responsibility: Marsh Youngbluth,
Fort Pierce, Florida, USA

Submitted: March 20, 2020; Accepted: August 10, 2020
Proofs received from author(s): September 25, 2020